JACS
JOURNAL OF THE AMERICAN CHEMICAL SOCIETY
Article
pubs.acs.org/JACS

Enthalpic Signature of Methonium Desolvation Revealed in a Synthetic Host–Guest System Based on Cucurbit[7]uril

Yi Wang,[§] Jason R. King,[∥] Pan Wu,[∥] Daniel L. Pelzman,[§] David N. Beratan,*[,∥,#,§] and Eric J. Toone*[,∥,§]

[§]Department of Biochemistry, Duke University Medical Center, Durham, North Carolina 27710, United States
[∥]Department of Chemistry and [#]Department of Physics, Duke University, Durham, North Carolina 27708, United States

Supporting Information

ABSTRACT: Methonium (N^+Me_3) is an organic cation widely distributed in biological systems. As an organic cation, the binding of methonium to protein receptors requires the removal of a positive charge from water. The appearance of methonium in biological transmitters and receptors seems at odds with the large unfavorable desolvation free energy reported for tetramethylammonium (TMA^+), a frequently utilized surrogate of methonium. Here, we report an experimental system that facilitates incremental internalization of methonium within the molecular cavity of cucurbit[7]uril (CB[7]). Using a combination of experimental and computational studies, we show that the transfer of methonium from bulk water (partially solvated methonium state) to the CB[7] cavity (mostly desolvated methonium state) is accompanied by a remarkably small desolvation enthalpy of just 0.5 ± 0.3 kcal·mol^{-1}, a value significantly less endothermic than those values suggested from gas-phase model studies. Our results are in accord with neutron scattering measurements that suggest methonium produces only a minimal perturbation in the bulk water structure, which highlights the limitations of gas-phase models. More surprisingly, the incremental withdrawal of the methonium surface from water produces a nonmonotonic response in desolvation enthalpy. A partially desolvated state exists, in which a portion of the methonium group remains exposed to solvent. This structure incurs an increased enthalpic penalty of ∼3 kcal·mol^{-1} compared to other solvation states. We attribute this observation to the pre-encapsulation dewetting of the methonium surface. Together, our results offer a rationale for the wide distribution of methonium in a biological context and suggest limitations to computational estimates of binding affinities based on simple parametrization of solvent-accessible surface area.

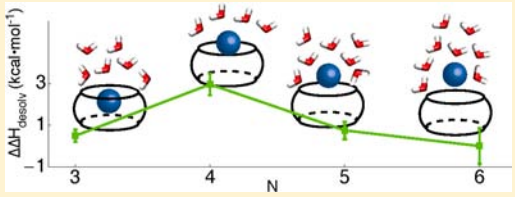

INTRODUCTION

Trimethylammonium (N^+Me_3; methonium) is an amphiphilic cation broadly distributed in biology, playing roles in processes as diverse as neurotransmission and lipid bilayer formation. Methonium-binding proteins often include binding sites that segregate the positively charged quaternary ammonium ion from bulk water.[1−5] Although many metal-binding proteins sequester inorganic cations using electron-rich residues such as histidine or ionized organic acids such as aspartate and glutamate,[6,7] binding sites that accommodate methonium typically lack anionic moieties capable of forming strong electrostatic interactions.[2−5,8] Rather, the most prevalent structural motif observed in methonium binding sites of proteins is an aromatic cage that forms cation−π interactions with the ligand.[9]

The means by which proteins bind methonium with a net favorable free energy is unclear. Cation−π interactions are weak: calculated and experimental values for the gas-phase interaction energy between tetramethylammonium (TMA^+), a surrogate for methonium in many biophysical studies, and benzene range from −4 to −9 kcal·mol^{-1}.[10−13] Yet, the measured desolvation free energy of TMA^+ is +38.3 kcal·mol^{-1}, dominated by a large unfavorable desolvation enthalpy of +49.3 kcal·mol^{-1} at 298 K.[14,15] These data suggest that the transfer of methonium from water to a hydrophobic binding pocket should produce large enthalpic and free energetic costs for binding. Even with four aromatic residues, the maximum number of aromatic rings geometrically capable of forming direct contact with methonium,[16] the energy available from cation−π interactions is too small to offset the +49.3 kcal·mol^{-1} enthalpic cost of methonium desolvation.

In contrast to gas-phase aqueous transfer thermodynamic parameters for TMA^+, a number of recent biophysical studies suggest that both free TMA^+ and methonium may be only weakly solvated.[17,18] Hulme and co-workers studied the hydration of acetylcholine and observed a water structure that precludes significant charge-dipole interaction between water and the methonium group.[19] Rather, charge transfer to the methyl hydrogen atoms produces a large, diffuse charged species that interacts only weakly with water.[20,21] Further, sites designed to accommodate methonium are unable to accommodate similarly sized inorganic cations. Thus for example, acetylcholine esterase crystals soaked in CsCl show no evidence of Cs^+ occupancy in the binding pocket,[22] despite the fact that Cs^+ and TMA^+ have similar sizes[23] and similar gas-phase water transfer thermodynamics.[14,15] Rather, the authors suggested that weak methonium solvation relative to inorganic cations

Received: November 18, 2012
Published: March 19, 2013

   dx.doi.org/10.1021/ja311327v | J. Am. Chem. Soc. 2013, 135, 6084−6091

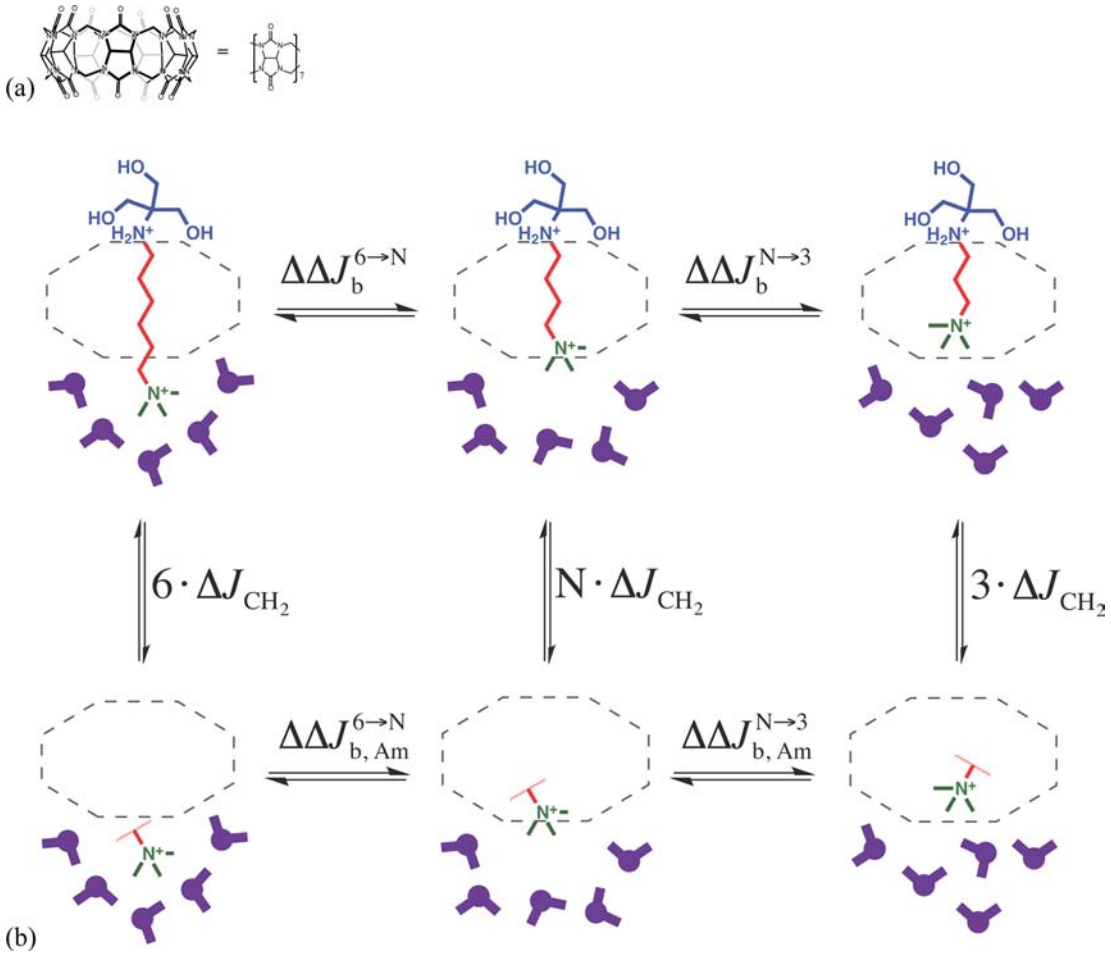

Figure 1. Model system for ligand binding (upper row): (a) CB[7] serves as a synthetic host for the ligands. (b) The ligands are composed of three regions: the Tris anchor (blue) that stabilizes each ligand in the series in the same geometry for binding and the alkyl linker (red) which varies the length of the ligand to affect the solvation of the methonium (green). Methonium is repositioned with respect to the cavity of CB[7] (dotted outline) as the linker length is varied. The ligand binds to CB[7] through the center of the torus. The change in binding thermodynamics upon shortening of the linker ($\Delta\Delta J_b^{6\to N}$) is monitored via ITC. By correcting $\Delta\Delta J_b^{6\to N}$ with the per-methylene contribution (ΔJ_{CH_2}) from the study of the CB[7]·**1** complexes, we obtain $\Delta\Delta J_{b,Am}^{6\to N}$ which is the net change in thermodynamic parameters when methonium moves toward a predesolvated nonpolar cavity (water: purple).

may facilitate desolvation and binding of methonium in a hydrophobic binding site.

Despite compelling structural evidence from neutron scattering studies that methonium may in fact be only loosely bound to water, thermodynamic evidence for such weak interactions is absent. Simple binding studies of TMA^+ and acetylcholine binding to proteins or synthetic hosts yield only aggregate binding thermodynamic data that contain contributions from both desolvation as well as solute−solute interactions of the entire ligand with the host. These data are of limited use for quantifying the thermodynamic consequences of desolvating individual functional groups, as pointed out by Diederich and others.[21,24−26]

To quantify the thermodynamic consequence of methonium group desolvation upon encapsulation in a simple molecular cavity, one has to accomplish two major tasks: (1) effectively separate the methonium−host binding thermodynamics from the contributions of the rest of the ligand; (2) determine the thermodynamics of solute−solute interactions separately from the desolvation effects upon binding.[27,28] To achieve the first goal, we devised an experimental system comprising a synthetic host, namely cucurbit[7]uril (CB[7], Figure 1a), and a series of guests in which the structure of bound complex, and consequently the extent of ligand desolvation, can be systematically altered by synthetic design. CB[7], a model receptor for protein−ligand complexes, sequesters methonium from aqueous solvent in a rigid, deep hydrophobic cavity.[21,27,29−31] The value of CB[7] for probing desolvation was described earlier by Mock and others.[32−36] In our approach here, we use two ligand series: (i) a reference series of 2-(hydroxymethyl)-2-(alkylamino)propane-1,3-diols (**1**) and (ii) a test series 2-((1,3-dihydroxy-2-(hydroxymethyl)propan-2-yl)amino)-*N*,*N*,*N*-trimethylalkaminium bromides (**2**; Figure 2). Ligand series **2**, comprising an anchor (Tris), a variable length tether (linear alkyl chain), and methonium, are bound to the host through the central cavity. With a tether of sufficient length, steric demands preclude sequestration of the

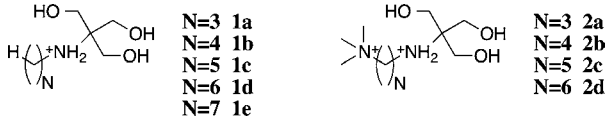

Figure 2. Chemical structure of ligand series **1** and **2**.

dx.doi.org/10.1021/ja311327v | *J. Am. Chem. Soc.* 2013, 135, 6084−6091

methonium group within the cavity but rather leave the charged organic cation outside of the CB[7] cavity and, at least partially, solvated. Introducing the anchor group locks the entire ligand with respect to the host, and systematic shortening of the tether gradually repositions the methonium group from water to the host interior, desolvating the epitope (Figure 1b).[32,36−38] We conducted thermodynamic analysis of CB[7]·**2** binding using isothermal titration microcalorimetry (ITC).

Following the additivity principle of Jencks and Page,[39,40] binding thermodynamic parameters as a function of linker length yield a thermodynamic difference ($\Delta\Delta J_b$, $J = G, H, S, C_p$) where $\Delta\Delta J_b$ is composed of two terms: a term attributable to linker variation ($\Delta\Delta J_{linker}$), and a term attributable to variation in the positioning of the terminal group, in this case methonium ($\Delta\Delta J_{b,Am}$). As the anchor moiety locks all ligands in a similar geometry when bound to the host, $\Delta\Delta J_{b,Am}$ can be extracted by comparison of ligand series **2** with a reference series of methyl-terminated ligands. As the terminal methonium group is absent in the reference series, $\Delta\Delta J_b$ of these ligands essentially arises completely from $\Delta\Delta J_{linker}$. Thermodynamic analysis of ligand series **1** binding to CB[7] thus facilitates determination of the net energetic consequences of partitioning methonium between water and the nonpolar cavity of CB[7] ($\Delta\Delta J_{b,Am}$), a feat unachievable with homobifunctional ligands such as the bis-ammonium alkanes reported by Mock and Shih.[32]

Currently available approaches to the second challenge, separation of solute−solute from solute−solvent binding thermodynamics, typically involve in silico estimation of the solute−solute interaction free energies and enthalpies, discounting solute−solvent interactions.[41,42] Thermodynamic analyses of various methonium-binding proteins suggest binding free energies that are dominated by the enthalpic component.[1,3,9] Therefore, as an initial step toward quantifying the methonium desolvation thermodynamic parameters, we used MD simulations to calculate the net change in methonium−CB[7] interaction enthalpy upon the incremental internalization of methonium ($\Delta\Delta H_{int,Am}$). Combining $\Delta\Delta H_{int,Am}$ with $\Delta\Delta H_{b,Am}$ obtained from ITC experiments, we estimate the enthalpic signature of methonium desolvation upon binding ($\Delta\Delta H_{desolv,Am} = \Delta\Delta H_{b,Am} - \Delta\Delta H_{int,Am}$).

We report the result of combined experimental and computational study here that the methonium group is only weakly solvated, incurring a smaller enthalpic penalty for desolvation than those derived from gas-phase studies of TMA^+, consistent with the suggestion of Hulme and coworkers.[19] Our result also offers a cautionary prescription for using standard desolvation thermodynamic parameters based on free homologues to describe the behavior of tethered functional groups and sheds light on the biophysical nature of choline-binding proteins and the energy landscape of epitope desolvation.

MATERIALS AND METHODS

General Syntheses. Synthesis, purification, and analysis of all ligands are reported in the Supporting Information. CB[7] was synthesized and purified according to literature procedure.[43]

^{1}H NMR Structural Studies. The ^{1}H NMR spectra of D_2O solutions containing roughly 8 mM CB[7] and 16 mM ligand was recorded on a Bruker 500 MHz NMR spectrometer. The exact ($[CB7]_{total}/[Lig]_{total}$) ratio was determined by peak integration. Complexation-induced shifts ($\Delta\delta$) were calculated based on the chemical shifts of the free ligand and equilibrium binding constant (K_a) measured with ITC. A detailed description of the protocol is provided in the Supporting Information.

Isothermal Titration Calorimetry. All titrations were carried out on a VP-ITC calorimeter (GE Healthcare). A typical ITC titration was carried out by titrating 30 aliquots of ligand solution (15 μL) into a CB[7] solution, with 350 s intervals between injections. Ligand concentrations were ∼12−15-fold greater than that of the CB[7] solutions, which in turn were set to ensure *c*-values remained between 1 and 1000. Data from all ITC titrations are provided in the Supporting Information.

Thermodynamic Model. We take a two-pronged approach to make an estimate of the desolvation enthalpy of methonium: (1) we separate the net thermodynamic effect of methonium encapsulation in the CB[7] cavity from the rest of the ligand matter; (2) we calculate the change of methonium−CB[7] interaction enthalpy to back out the solvation terms from experimental ITC results in aqueous solution. Our strategy for the first step follows from the anchor principle of group additivity,[39,40] and the linear free energy relationship theory of Schneider for synthetic host−guest complexes,[44] which postulates that contributions to the binding thermodynamic parameters (ΔJ_b, $J = G, H, S, C_p$) from the anchor, the linker, and the methonium group are additive. Our thermodynamic models are described briefly here; a more detailed derivation is provided in the Supporting Information. This model is illustrated in Figure 1, which shows that the binding of ligand series **2** to CB[7] can be effectively transformed into the binding of methonium to a predesolvated cavity.[45]

The CB[7]·**1** complexes were used to quantify the thermodynamic contribution of a methylene group, ΔJ_{CH_2}, to the overall binding thermodynamics. We applied a linear approximation by partitioning binding thermodynamic parameters as functions of the number of methylene groups in the linker (N):

$$\Delta J_b^{CB[7]\cdot\mathbf{1}} = \Delta J_{CH_2} N + \Delta J_0 \quad (1)$$

where ΔJ_{CH_2} is the thermodynamic effect per methylene group in the alkyl linker and can be determined numerically by data fitting.

We next define the difference in binding thermodynamics ($\Delta\Delta J_b^{6\to N}$) between ligands **2a−c** with a linker of three to five methylene groups ($\Delta J_b^{CB[7]\cdot\mathbf{2a-c}}$) and the reference ligand **2d** which contains a six methylene linker ($\Delta J_b^{CB[7]\cdot\mathbf{2d}}$), defining the CB[7]·**2d** complex as the reference state. Because the Tris anchor fixes the rest of the complex at a constant position, $\Delta\Delta J_b^{6\to N}$ contains contributions from change of the linker length, $(N\text{-}6)\Delta J_{CH_2}$, as well as a contribution associated with repositioning the methonium group from its equilibrium position in the CB[7]·**2d** complex to the corresponding position in the CB[7]·**2a−c** complexes ($\Delta\Delta J_{b,Am}^{6\to N}$, previously denoted as $\Delta\Delta J_{b,Am}$):

$$\Delta\Delta J_{b,Am}^{6\to N} = \Delta\Delta J_b^{6\to N} - (N-6)\Delta J_{CH_2} \quad (2)$$

$\Delta\Delta J_{b,Am}^{6\to N}$ consists of a desolvation term ($\Delta\Delta J_{desol,Am}^{6\to N}$) and terms representing contributions from intrinsic interactions ($\Delta\Delta J_{int,Am}^{6\to N}$):

$$\Delta\Delta J_{b,Am}^{6\to N} = \Delta\Delta J_{int,Am}^{6\to N} + \Delta\Delta J_{desolv,Am}^{6\to N} \quad (3)$$

In this study, $\Delta\Delta H_{int,Am}^{6\to N}$ (previously denoted as $\Delta\Delta H_{int,Am}$) was calculated via MD simulation based on eq 18 of the Supporting Information. Therefore, by experimentally determining $\Delta\Delta H_{b,Am}^{6\to N}$ via ITC, we can estimate $\Delta\Delta H_{desolv,Am}^{6\to N}$, that is the *net enthalpy change* for the incremental desolvation of methonium. Standard deviations of all terms were calculated by the propagation of experimental standard deviations.

Computations. The initial coordinates of CB[7] were taken from the published crystal structure.[46] Structures of ligands were generated using Chem3D (Cambridge Software), and the initial complex structures were created via molecular docking using AutoDock.[47] For the construction of atomistic models of the complexes, the highest ranking pose from docking analysis was geometry optimized using Gaussian 09 (Gaussian Inc.[48]) at a DFT/B3LYP[49]/6-31G basis level with an implicit solvent polarizable continuum model (PCM).[50]

dx.doi.org/10.1021/ja311327v | J. Am. Chem. Soc. 2013, 135, 6084−6091

To calculate $\Delta\Delta H^{6\rightarrow N}_{int,Am}$, we parametrized ligand series **2** using the force field tools kit (FFTk) in the VMD program; partial charges of the ligands were optimized at the HF/6-31G* level.[51] Valence parameters were taken either from the CHARMM general force field[52] based on homology or were optimized at the MP2/6-31G* level. All quantum chemical calculations were carried out using the Gaussian 09 program.[48] Partial charges and force-field parameters for CB[7] of Moghaddam et al. were used.[27] The solvent accessible surface area (SASA) of methonium is calculated as the ensemble average from MD simulation trajectories. Water occupancy maps were calculated using VMD.[51] Computational details are provided in the Supporting Information.

RESULTS AND DISCUSSION

Structural Validation of the CB[7]·1 and CB[7]·2 Systems. To implement our strategy of controllable internalization, we require an anchor moiety that cannot enter the central pore of CB[7] but that requires insertion of the linker and terminal epitope of the guest within the cavity. CB[7] perturbs the chemical shifts of bound protons, which is well established and provides a direct correlation between the ^{1}H NMR complexation-induced chemical shift ($\Delta\delta$) and the degree of internaliztion of these protons within CB[7].[29,31,53,54] A combination of ^{1}H NMR structural data and synthetic feasibility constraints supported the use of Tris as the anchor group. The hydroxymethyl protons of ligands **2a−d** show a consistent downfield shift ($\Delta\delta$ = 0.21 ± 0.03 ppm) upon binding, consistent with placement of the anchor group outside of the cavity in a constant position across the ligand series (Figure 3 and Supporting Information). The observed

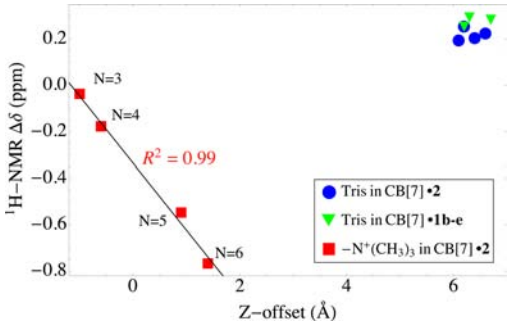

Figure 3. The ^{1}H NMR complexation-induced shift of Tris methylene and methonium methyl protons vs the Z-offsets of Tris N and methonium N from QM/MM simulations. Blue circles and green triangles depict the position of the Tris anchor group in line with the top portal of CB[7] (Z = 6 Å) in the probe series **2a−d** and reference ligand series **1b−e**, respectively. Red squares depict the relative position of the methonium epitope with respect to the lower portal of CB[7] (Z = 0 Å) with increasing linker length (top to bottom and left to right in the plot).

NMR shifts are in good agreement with those reported by Zhao and colleagues for alkylimidazolium ligands.[37] On the other hand, methonium protons undergo an increasing upfield shift as the alkyl linker is shortened, confirming that the locked position of the Tris anchor "pulls" the X-group into the cavity. Hydroxymethyl protons in the CB[7]·**1b−e** complexes consistently shift downfield upon binding in a fashion similar to those of the CB[7]·**2** complexes (Figure 3 and Supporting Information), highlighting again the powerful ability of the Tris anchor group to define the positions of guests within the host. Ligand **1a** binds CB[7] in a structurally distinct fashion from the other members of the series with the Tris anchor encapsulated (Supporting Information) and was removed from the study.

To further verify the complex structures of our design, we computed energy-minimized structures of the CB[7]·**2a−d** and CB[7]·**1b−e** complexes using QM/MM simulations with explicit solvent (Figure 4 and Supporting Information). The

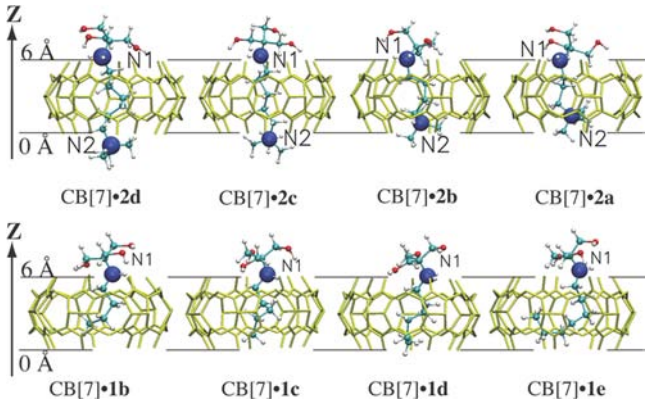

Figure 4. The complex structures of CB[7]·**2** and CB[7]·**1b−e** generated via DFT geometry optimization with implicit solvent. N1 (blue ball) denotes the nitrogen atom of the anchor group. N2 (blue ball) denotes the nitrogen atom of methonium. Hydrogen atoms on CB[7] are omitted for clarity.

axis of rotational symmetry of CB[7] defines the Z-axis, and the seven lower portal oxygen atoms were placed at Z = 0 Å. The computed offsets of N1 (Tris) and N2 (methonium, **2a−d**) along the Z-axis are shown in Table 1. N1 in all complexes is

Table 1. Binding Thermodynamics of the CB[7]·1 Complexes at 298 K[a]

	N	ΔG_b	ΔH_b	$T\Delta S_b$
CB[7]·**1b**	4	−5.4 ± 0.1	0.8 ± 0.2	6.2 ± 0.2
CB[7]·**1c**	5	−7.2 ± 0.1	−1.2 ± 0.0	5.9 ± 0.0
CB[7]·**1d**	6	−8.0 ± 0.1	−3.1 ± 0.1	4.9 ± 0.1
CB[7]·**1e**	7	−8.1 ± 0.0	−3.7 ± 0.0	4.3 ± 0.1

[a]Units: kcal·mol^{-1}.

located above the upper portal of the CB[7] host with minimal Z-axis variation, in contrast to a significant change of N2 along the Z-axis across the series **2d** to **2a**. The trends of the N1 and N2 Z-offsets agree well with chemical shift trends for Tris-methylene and methonium protons (Figure 3 and Supporting Information).

We attribute the anchoring ability of Tris to the hydrophilicity of the hydroxymethyl groups, which was supported by the study of two similarly sized anchor groups (Supporting Information). Hydrophilic anchor groups tend to remain in direct contact with the bulk water rather than to desolvate and enter the hydrophobic cavity of CB[7]. Experimental evidence from a series of negative controls (i.e., other anchors that are internalized; see Supporting Information) in conjunction with excellent agreement between experimental and theoretical values of ligand positions within CB[7] provide strong support for the view that the position of the Tris anchor remains constant across the ligand series. This idea is visualized by plotting the calculated change in position vs observed chemical shifts for the Tris anchor and internalized methonium (Figure 3). The ability of the Tris anchor to lock guests in a fixed

dx.doi.org/10.1021/ja311327v | J. Am. Chem. Soc. 2013, 135, 6084−6091

geometry serves as the foundation for the thermodynamic model.

Results from ^{1}H NMR studies suggest that the terminal methyl group of the CB[7]·**1** complexes remain inside the cavity regardless of linker length, an observation consistent with the energy-minimized structures. In the CB[7]·**1e** complex, the alkyl linker folds inside the cavity (Figure 4), giving rise to a destabilizing C4−C7 gauche interaction (Supporting Information), which was taken into account in the following thermodynamic analyses. In both the CB[7]·**2** and CB[7]·**1b−e** complexes, the alkyl linkers adopt helical conformations, similar to the geometries observed in cavitand−alkane complexes.[55] As previously described by Rebek and co-workers, the helical structure most likely results from the propensity of the alkyl chain to reduce solvent exposure and to fill the cavity volume.[56]

Determination of ΔJ_{CH_2} by ITC. Thermodynamic parameters for the formation of the CB[7]·**1b−e** complexes[57] (Table 1) indicate that binding is entropically driven with a favorable (negative) $\Delta H_b^{CB[7]\cdot 1}$ for **1c−1e** and an unfavorable $\Delta H_b^{CB[7]\cdot 1}$ for **1b**. We treat each value of ΔJ_b as a linear function of N to estimate the per-methylene contribution (ΔJ_{CH_2}) of the linker to ΔJ_b. In accordance with the QM-optimized structure of the CB[7]·**1e** complex, a C4−C7 gauche interaction resulted in a 1.3 kcal·mol^{-1} deviation from the linear trend observed for ligands **1b−d** (Figure 5). Accordingly, we only use data for

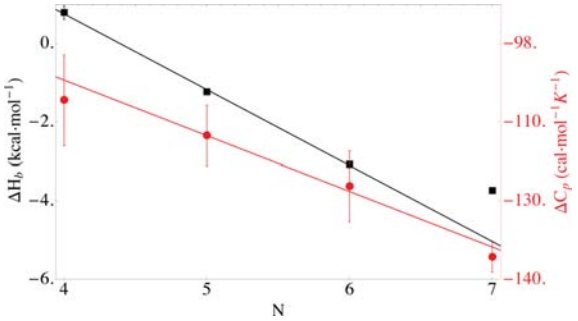

Figure 5. The binding enthalpy (298 K) and heat capacity of the CB[7]·**1** complexes. Black squares: ΔH; red circles: ΔC_p. Error bars for ΔH are of similar scale to the size of the symbols. The linear fit of ΔH includes only **1b−d**; the linear fit for ΔC_p includes **1b−e**. See the Supporting Information for details of the linear regressions.

ligands **1b−d** to extract ΔH_{CH_2} (−1.9 ± 0.1 kcal·mol^{-1}), ΔG_{CH_2} (−1.3 ± 0.3 kcal·mol^{-1}), and ΔS_{CH_2} (−0.6 ± 0.2 kcal·mol^{-1} at 298 K). As expected, the enthalpic cost of the solvent-independent gauche interaction does not translate into $\Delta C_p^{CB[7]\cdot 1}$, and a clear linear correlation with N is observed across the entire series **1b** to **1e** (Figure 5). The slope of this plot provides a per-methylene contribution (ΔC_p^{CH2}) of −11 ± 2 cal·mol^{-1}·K^{-1}, in good accord with previously reported values of −15 cal·mol^{-1}·K^{-1}.[58,59] This correlation validates two critical assumptions: (1) heat capacity changes are dominated by desolvation changes upon binding; and (2) the energetic contribution from desolvation of the alkyl linker varies linearly across the entire series **1b** to **1e**, regardless of the conformation adopted by the ligand in the bound form.

Enthalpy of Desolvation of Tethered Methonium. Table 2 shows thermodynamic parameters for the binding of ligands **2a−d** ($\Delta J_b^{CB[7]\cdot 2a-d}$) at 298 K, which show that the binding of ligand series **2** to CB[7] is entropically driven. However, after correction for the linker contribution (eq 2), it is clear that methonium encapsulation is enthalpically driven (Table 2), in good accord with previous studies.[1,3,9,21] The transfer of methonium from bulk water to the hydrophobic cavity of CB[7] is spontaneous ($\Delta G_{b,Am}^{6\to 3}$ = −1.7 kcal·mol^{-1}), driven by a negative (favorable) enthalpy change ($\Delta H_{b,Am}^{6\to 3}$ = −4.0 kcal·mol^{-1}) and accompanied by an unfavorable entropy change ($\Delta S_{b,Am}^{6\to 3}$ = −8 cal/mol·K). $\Delta H_{int,Am}^{6\to N}$ from MD simulations of the CB[7]·**2** complexes (eq 18 of Supporting Information) enable determination of the enthalpy of desolvation with respect to methonium encapsulation ($\Delta\Delta H_{desolv,Am}^{6\to N}$). Figure 6a shows the correlation between $\Delta\Delta H_{b,Am}^{6\to N}$, $\Delta\Delta H_{int,Am}^{6\to N}$, and $\Delta\Delta H_{desolv,Am}^{6\to N}$ as a function of the change in the ensemble averaged SASA relative to the N = 6 state (ΔSASA). The binding of methonium to the CB[7] cavity produces a negative enthalpy change, presumably derived from favorable methonium−CB[7] interactions (N = 6 to N = 4). A large favorable change in binding enthalpy is observed as the linker is shortened from N = 4 to N = 3 ($\Delta\Delta H_{b,Am}^{4\to 3}$). Because the CB[7]−methonium interactions are similar in both ligands, this shift presumably arises from changes in desolvation enthalpy. The unfavorable net change in desolvation ($\Delta\Delta H_{desolv,Am}^{6\to N}$) correlates no more than weakly with the change in SASA, with a maximum observed at N = 4. At least two explanations rationalize this observation.

First, energetic terms for which our thermodynamic model does not account, such as changes in the internal energy of the ligand or the receptor across the series, may manifest themselves in the derived values of $\Delta\Delta H_{desolv,Am}^{6\to N}$. Shortening of the linker from N = 5 to N = 4 begins to draw methonium into the cavity. The equilibrium diameters of the CB[7] portal and methonium are ∼4−5 Å and ∼5−6 Å, respectively.[46] Thus, at the equilibrium position of methonium in the CB[7]·**2b** (N = 4) complex, the CB[7] portal may undergo distortion to accommodate the methonium group, or geometric constraints may force the methonium group to move further into or out of the cavity than would be predicted purely on the basis of linker length, incurring strain in the alkyl linker. Any of these effects, albeit no more than minor, would negate the simplifying assumptions of our thermodynamic model, producing additional destabilizing enthalpic contributions to the apparent $\Delta\Delta H_{desolv,Am}^{6\to N}$. At a minimum, structural distortions of the CB[7] cavity arising from methonium encapsultion were not

Table 2. Binding Thermodynamics of the CB[7]·2 Complexes at 298 K[a]

	N	ΔG_b	ΔH_b	$T\Delta S_b$	$\Delta\Delta G_{b,Am}^{6\to N}$	$\Delta\Delta H_{b,Am}^{6\to N}$	$T\Delta\Delta S_{b,Am}^{6\to N}$
CB[7]·**2a**	3	−6.8 ± 0.1	−0.6 ± 0.1	6.2 ± 0.1	−1.7 ± 1.0	−4.0 ± 0.3	−2.3 ± 0.9
CB[7]·**2b**	4	−7.2[b]	−0.1[b]	7.1[b]	−0.8 ± 0.7	−1.5 ± 0.2	−0.8 ± 0.6
CB[7]·**2c**	5	−8.1 ± 0.0	−1.5 ± 0.0	6.5 ± 0.0	−0.3 ± 0.3	−1.0 ± 0.1	−0.8 ± 0.3
CB[7]·**2d**	6	−9.1 ± 0.0	−2.4 ± 0.1	6.7 ± 0.1	0.0 ± 0.2	0.0 ± 0.1	0.0 ± 0.1

[a]Units: kcal·mol^{-1}. [b]These values were extrapolated from thermodynamic data at other temperatures.

dx.doi.org/10.1021/ja311327v | J. Am. Chem. Soc. 2013, 135, 6084−6091

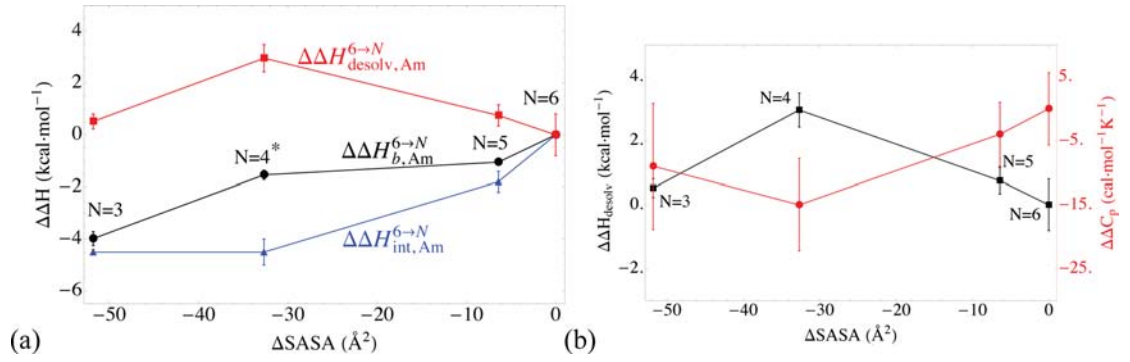

Figure 6. (a) The net enthalpic effect of moving the methonium group from solvent ($N = 6$) to the cavity ($N = 3$), is plotted against ΔSASA at 298 K. N (black) is the number of methylene groups in the linker. Black circle: $\Delta\Delta H^{6\to N}_{b,Am}$; blue triangle: $\Delta\Delta H^{6\to N}_{int,Am}$; red square: $\Delta\Delta H^{6\to N}_{desolv,Am}$. *$\Delta\Delta H^{6\to 4}_{b,Am}$ at 298 K was obtained by extrapolating $\Delta H^{CB[7]\cdot 2b}_{b}$ from the enthalpic data at other temperatures due to a near-zero enthalpy at 298 K. (b) $\Delta\Delta C^{6\to N}_{p,Am}$ (red circle) and $\Delta\Delta H^{6\to N}_{desolv,Am}$ (black square) vs the net change of methonium SASA (ΔSASA).

apparent in a superposition of the QM-calculated complex structures, depicting RMS differences no greater than 0.2 Å for CB[7] structures throughout the CB[7]·**2** series.

A second more intriguing possibility is that $\Delta\Delta H^{6\to N}_{desolv,Am}$ does not vary monotonically with the solvent-exposed surface area, in which case the nonlinearity in Figure 6a is representative of a more complex desolvation energy landscape. Similar effects (in silico) have been discussed in the context of hydrophobic desolvation during helix formation[60] and the binding of a methane-sized particle in a hydrophobic cavity.[61,62] Fortunately, these two possibilities are experimentally distinguishable: solvation-associated contributions to binding enthalpies are temperature dependent while the solute−solute interactions and configurational enthalpies are temperature independent.[63,64] We can thus differentiate the possibilities by evaluating the changes in isobaric heat capacity that occur upon shortening of the linker and concomitant methonium encapsulation in CB[7] ($\Delta\Delta C^{6\to N}_{p,Am}$).

Heat Capacity as a Measure of Solvent Reorganization. Figure 6b shows the correlation of $\Delta\Delta C^{6\to N}_{p,Am}$ and $\Delta\Delta H^{6\to N}_{desolv,Am}$ with ΔSASA. Similar to $\Delta\Delta H^{6\to N}_{desolv,Am}$, $\Delta\Delta C^{6\to N}_{p,Am}$ does not follow a simple monotonic trend but rather shows an apparent minimum at $N = 4$. Propagation and accumulation of errors in $\Delta\Delta C^{6\to N}_{p,Am}$ preclude precise assessment of the heat capacity changes associated with methonium transfer into the cavity of CB[7]. Nonetheless, a discontinuity in $\Delta\Delta C^{6\to N}_{p,Am}$ at $N = 4$ qualitatively coincides with the maximum observed in $\Delta\Delta H^{6\to N}_{desolv,Am}$ prior to complete methonium encapsulation. In light of the absence of significant distortion of CB[7] for $N = 4$ (vide supra), the observed $\Delta\Delta C^{6\to N}_{p,Am}$ supports the notion that an unfavorable enthalpic component for $N = 4$ arises from solvent reorganization rather than from increased torsional strain in the CB[7]·**2** complexes. Also consistent with this hypothesis are earlier computational studies that predicted a nonmonotonic trend of desolvation enthalpy with decreasing intermolecular distance upon the association of nonpolar surfaces in water.[65]

The nonmonotonic nature of the $\Delta\Delta H^{6\to N}_{desolv,Am}$ and $\Delta\Delta C^{6\to N}_{p,Am}$ plots prevents unambiguous determination of the desolvation enthalpy of a fully solvated methonium by linear extrapolation (SASA = 167 Å^2). However, given an exceptionally small enthalpy change in the partial desolvation of methonium ($\Delta\Delta H^{6\to 3}_{desolv,Am} = 0.5 \pm 0.3$ kcal·mol^{-1}), it appears highly unlikely that the enthalpic penalty for transfer of the full methonium surface from water to a hydrophobic cavity will be close to the gas-phase value for TMA^+ desolvation enthalpy (+49 kcal·mol^{-1}). On the other hand, our results are not necessarily inconsistent with TMA^+ gas-phase data. An intriguing explanation for this discrepancy is that methonium retains significant stabilizing interactions with bulk water even when encapsulated in the CB[7] pore. Even upon full encapsulation ($N = 3$), methonium is only separated from the nearest water molecules by the 6−8 Å wall of CB[7] cavity. The low dielectric constant of the CB[7] structure may enable strong methonium−water electrostatic interactions. In contrast to gas-phase studies, where the water−TMA^+ electrostatic interactions disappear upon removal of solute, these interactions may be substantially retained even after the transfer of methonium from water to the CB[7] cavity, giving rise to the diminished enthalpic penalty of desolvation.

A review of methonium binding proteins shows that methonium is typically removed from bulk water by less than 20 Å, albeit in a pocket surrounded by aromatic moieties.[1−5,66] The enthalpic behavior of methonium desolvation observed here may reflect Nature's strategy for methonium binding in proteins; although methonium is *desolvated* in the sense that it lacks direct *physical* contact with water, the charge it carries remains in *electrostatic* contact with solvent, a situation starkly different from that in gas phase-studies. As a result, the large enthalpic penalty found in gas-phase studies may be mitigated in the binding of methonium to CB[7] and other receptors because of indirect interactions with solvent. This postulate warrants further testing.

Occupancy Maps of Solvation Shell Water of Methonium. To further understand the nonlinearity in our energy-surface plots, we calculated local occupancy maps for water surrounding methonium in the CB[7]·**2** complexes (Figure 7) based on the MD simulation trajectories. The first solvation shell of the solvated states (Figure 7) has a water occupancy higher than that of the bulk. Collapse of this first solvation shell takes place well before methonium enters the cavity (from $N = 5$ to $N = 4$), an observation consistent with the results of McCammon and others.[60−62] At $N = 4$, the first solvation shell of methonium nearly vanishes, *prior* to full encapsulation at $N = 3$. Disruption of the solvation shell upon binding was shown to be unfavorable enthalpically[61,62,67] and may explain the observed trend in desolvation thermodynamic parameters: the low-occupancy region near methonium in the CB[7]·**2b** complex contains energetically perturbed waters (relative to the bulk) that produce both the enthalpic

dx.doi.org/10.1021/ja311327v | J. Am. Chem. Soc. 2013, 135, 6084−6091

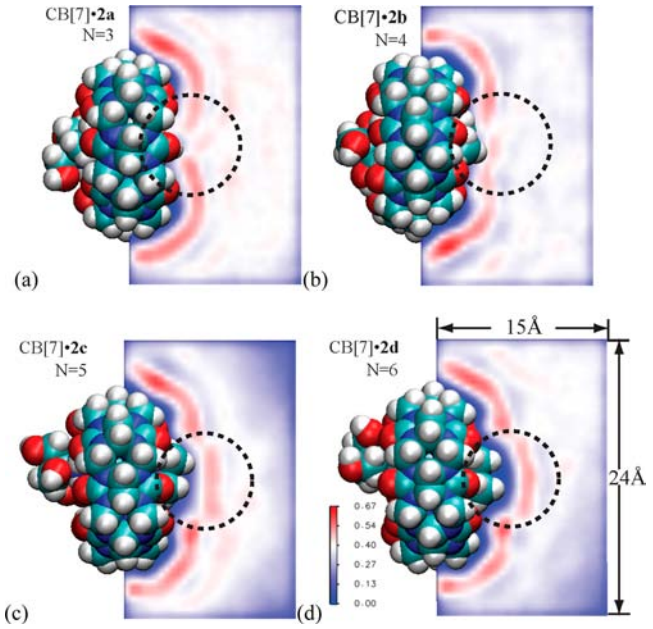

Figure 7. Local occupancy maps of water in a 15 Å × 24 Å × 0.24 Å slice passing through the center of methonium N atom and perpendicular to the CB[7]-portal. Molecular graphics were produced by using VMD: (a) CB[7]·**2a**; (b) CB[7]·**2b**; (c) CB[7]·**2c**; (d) CB[7]·**2d**. Dashed circles highlight the disappearance of the first solvation shell of methonium from d to a.

discontinuity at N = 4 and the minimum in $\Delta\Delta C_{p,Am}^{6\rightarrow N}$. The release of this so-called activated water[68] to the bulk liberates $-\Delta\Delta H_{desolv,Am}^{4\rightarrow 3} \approx$ 2.5 kcal·mol^{-1} at 298 K. Although the enthalpic maximum at N = 4 may be due to the unique curvature of the surface constituted by the CB[7] portal and methonium,[69,70] the observation of perturbed water is common in both biological and abiological systems.[67,71,72] At the very least, the presence of a complex desolvation energy landscape for the CB[7]·**2b** complex calls into question the validity of using simple water to either gas phase or octanol partition coefficients to assign the energetic contributions of water for ligand binding in aqueous solution.

CONCLUSIONS

We used a unique host−guest system comprising CB[7] and a series of de novo designed ligands to determine the thermodynamics of methonium desolvation and binding to a hydrophobic cavity. In this system, a Tris anchor fixes a ligand in place with respect to the host, and methonium is incrementally repositioned from bulk water into the cavity by shortening an alkyl linker. The transfer of methonium from the partially solvated state of the N = 6 ligand to the fully encapsulated state at N = 3 is driven by exothermic methonium−CB[7] interactions. The data presented here furnish evidence that the desolvation of methonium occurs with a significantly diminished enthalpic penalty relative to the gas-phase desolvation of TMA$^+$. The small values of heat capacity changes that accompany binding suggest minimal solvent reorganization upon encapsulation of methonium, consistent with neutron scattering studies that show a remarkably unperturbed solvation shell around the methonium ion.[19]

More importantly, our approach of incremental internalization revealed nonmonotonic trends in both $\Delta\Delta C_{p,Am}^{6\rightarrow N}$ and $\Delta\Delta H_{desolv,Am}^{6\rightarrow N}$ as a function of methonium SASA, which echoes the arguments of Lemieux, Dill, and others that not all surface is created equal and approaches to parametrize desolvation thermodynamics based solely on SASA have serious limitations.[69−71] For a surface as simple as that of methonium, the enthalpic signature of binding desolvation depends strongly on the molecular topology of the surface formed by both the ligand and the receptor. The thermodynamic consequences of methonium binding to different receptor surfaces may be different despite the fact that equal SASA is desolvated. Our result reflects the common limitation of SASA-based thermodynamic analysis, namely that they operate well across a homologous series but fail on transfer to settings other than that from which the parameters are generated. As such, new methods of capturing relevant desolvation thermodynamic parameters for association in aqueous solution are needed for more accurate modeling of aqueous desolvation, a notion recently articulated by Baldwin.[73]

In any event, spontaneity of desolvating methonium from water is determined by the free energy of transfer into the cavity of CB[7]. The thermodynamic model developed here for enthalpy may not apply to free energy analysis, as the additive partitioning of $\Delta\Delta S_b^{CB[7]\cdot \mathbf{2a-d}}$ may not be valid. Gas-phase measurements of binding free energies and enthalpies in CB[n] systems offer an attractive means for establishing a free energy description of methonium desolvation, which was recently reviewed by Yang and Dearden.[74] We are currently exploring this approach.

Finally, we note that the study described here only accesses half of the total SASA of methonium. Indeed, the SASA of a fully solvated methonium group is 167 Å^2, while the most solvent-exposed state of methonium in the CB[7]·**2** complexes (N = 6) presents roughly half of this area to solvent. The correlation plots of $\Delta\Delta C_{p,Am}^{6\rightarrow N}$ and $\Delta\Delta H_{desolv,Am}^{6\rightarrow N}$ may represent asymptotic regions of two much steeper curves, and the desolvation of the entire 167 Å^2 SASA of methonium may entail a much greater enthalpic penalty than suggested by our data. Due to the flexible nature of the alkyl linker, however, the current design is unsuitable for probing more solvent-exposed states of methonium. Future studies using alkynyl or alkenyl linkers to extend the methonium further into the solvent may access a wider range of solvent-accessible states of methonium.

ASSOCIATED CONTENT

Supporting Information

Synthesis and characterization of CB[7] and all the ligands, NMR spectra of complexes, original data from ITC experiments, and detailed derivation of thermodynamic models. This material is available free of charge via the Internet at http://pubs.acs.org.

AUTHOR INFORMATION

Corresponding Author

david.beratan@duke.edu; eric.toone@duke.edu

Notes

The authors declare no competing financial interest.

ACKNOWLEDGMENTS

We thank Dr. Lyle Issacs at the University of Maryland for help in the preparation of CB[7]. We thank Dr. Xiaofei Liang for help in synthesis. We thank Dr. Xiangqian Hu for outstanding technical advice. We thank Dr. Terry Oas for fruitful discussion

of the project, and Dr. David Minh for discussion of the thermodynamic model. We thank the University of Pittsburgh Center for Chemical Methodologies and Library Development, through NIH grant P50 GM067082, for partial support of this project.

REFERENCES

(1) Bourne, Y.; Taylor, P.; Marchot, P. *Cell* **1995**, *83*, 503.
(2) Sixma, T. K.; Smit, A. B. *Annu. Rev. Biophys. Biomol. Struct.* **2003**, *32*, 311.
(3) Celie, P. H. N.; van Rossum-Fikkert, S. E.; van Dijk, W. J.; Brejc, K.; Smit, A. B.; Sixma, T. K. *Neuron* **2004**, *41*, 907.
(4) Pan, J.; Chen, Q.; Willenbring, D.; Yoshida, K.; Tillman, T.; Kashlan, O. B.; Cohen, A.; Kong, X. P.; Xu, Y.; Tang, P. *Nat. Commun.* **2012**, *3*, 714.
(5) Bourne, Y.; Radic, Z.; Sulzenbacher, G.; Kim, E.; Taylor, P.; Marchot, P. *J. Biol. Chem.* **2006**, *281*, 29256.
(6) Dudev, T.; Lim, C. *Annu. Rev. Biophys.* **2008**, *37*, 97.
(7) Celio, M. R.; Pauls, T. L.; Schwaller, B. *Guidebook to the calcium-binding proteins*; Sambrook & Tooze Publication at Oxford University Press: Oxford, 1996.
(8) Malito, E.; Sekulic, N.; Too, W. C.; Konrad, M.; Lavie, A. *J. Mol. Biol.* **2006**, *364*, 136.
(9) Karlin, A. *Nat. Rev. Neurosci.* **2002**, *3*, 102.
(10) Duffy, E. M.; Kowalczyk, P. J.; Jorgensen, W. L. *J. Am. Chem. Soc.* **1993**, *115*, 9271.
(11) Gao, J.; Chou, L. W.; Auerbach, A. *Biophys. J.* **1993**, *65*, 43.
(12) Felder, C.; Jiang, H. L.; Zhu, W. L.; Chen, K. X.; Silman, I.; Botti, S. A.; Sussman, J. L. *J. Phys. Chem. A* **2001**, *105*, 1326.
(13) Meotner, M.; Deakyne, C. A. *J. Am. Chem. Soc.* **1985**, *107*, 469.
(14) Marcus, Y. *J. Chem. Soc., Faraday Trans. 1* **1987**, *83*, 339.
(15) Marcus, Y. *J. Chem. Soc., Faraday Trans.* **1991**, *87*, 2995.
(16) Roelens, S.; Torriti, R. *J. Am. Chem. Soc.* **1998**, *120*, 12443.
(17) Turner, J.; Soper, A. K.; Finney, J. L. *Mol. Phys.* **1990**, *70*, 679.
(18) Turner, J.; Soper, A. K.; Finney, J. L. *Mol. Phys.* **1992**, *77*, 411.
(19) Hulme, E. C.; Soper, A. K.; McLain, S. E.; Finney, J. L. *Biophys. J.* **2006**, *91*, 2371.
(20) Parker, D.; Kataky, R.; Kelly, P. M.; Palmer, S. *Pure Appl. Chem.* **1996**, *68*, 1219.
(21) St-Jacques, A. D.; Wyman, I. W.; Macartney, D. H. *Chem. Commun. (Cambridge, U. K.)* **2008**, 4936.
(22) Dvir, H.; Silman, I.; Harel, M.; Rosenberry, T. L.; Sussman, J. L. *Chem.-Biol. Interact.* **2010**, *187*, 10.
(23) Barthel, J.; Krienke, H.; Kunz, W. *Physical chemistry of electrolyte solutions: modern aspects*; Steinkopff, Springer: Darmstadt, NY, 1998.
(24) Maelicke, A.; Fulpius, B. W.; Klett, R. P.; Reich, E. *J. Biol. Chem.* **1977**, *252*, 4811.
(25) Meyer, E. A.; Castellano, R. K.; Diederich, F. *Angew. Chem., Int. Ed.* **2003**, *42*, 1210.
(26) Bissantz, C.; Kuhn, B.; Stahl, M. *J. Med. Chem.* **2010**, *53*, 5061.
(27) Moghaddam, S.; Inoue, Y.; Gilson, M. K. *J. Am. Chem. Soc.* **2009**, *131*, 4012.
(28) Rauwald, U.; Biedermann, F.; Deroo, S.; Robinson, C. V.; Scherman, O. A. *J. Phys. Chem. B* **2010**, *114*, 8606.
(29) Lagona, J.; Mukhopadhyay, P.; Chakrabarti, S.; Isaacs, L. *Angew. Chem., Int. Ed.* **2005**, *44*, 4844.
(30) Schneider, H. J. *Angew. Chem., Int. Ed.* **2009**, *48*, 3924.
(31) Wyman, I. W.; Macartney, D. H. *Org. Biomol. Chem.* **2008**, *6*, 1796.
(32) Mock, W. L.; Shih, N. Y. *J. Org. Chem.* **1986**, *51*, 4440.
(33) Nau, W. M.; Florea, M.; Assaf, K. I. *Isr. J. Chem.* **2011**, *51*, 559.
(34) Biedermann, F.; Uzunova, V. D.; Scherman, O. A.; Nau, W. M.; De Simone, A. *J. Am. Chem. Soc.* **2012**, *134*, 15318.
(35) Nguyen, C. N.; Kurtzman Young, T.; Gilson, M. K. *J. Chem. Phys.* **2012**, *137*, 044101.
(36) Masson, E.; Ling, X. X.; Joseph, R.; Kyeremeh-Mensah, L.; Lu, X. Y. *RSC Adv* **2012**, *2*, 1213.
(37) Zhao, N.; Liu, L.; Biedermann, F.; Scherman, O. A. *Chem-Asian J.* **2010**, *5*, 530.
(38) Mukhopadhyay, P.; Zavalij, P. Y.; Isaacs, L. *J. Am. Chem. Soc.* **2006**, *128*, 14093.
(39) Page, M. I.; Jencks, W. P. *Proc. Natl. Acad. Sci. U.S.A.* **1971**, *68*, 1678.
(40) Jencks, W. P. *Proc. Natl. Acad. Sci. U.S.A.* **1981**, *78*, 4046.
(41) Moghaddam, S.; Yang, C.; Rekharsky, M.; Ko, Y. H.; Kim, K.; Inoue, Y.; Gilson, M. K. *J. Am. Chem. Soc.* **2011**, *133*, 3570.
(42) Rekharsky, M. V.; Mori, T.; Yang, C.; Ko, Y. H.; Selvapalam, N.; Kim, H.; Sobransingh, D.; Kaifer, A. E.; Liu, S. M.; Isaacs, L.; Chen, W.; Moghaddam, S.; Gilson, M. K.; Kim, K. M.; Inoue, Y. *Proc. Natl. Acad. Sci. U.S.A.* **2007**, *104*, 20737.
(43) Day, A.; Arnold, A. P.; Blanch, R. J.; Snushall, B. *J. Org. Chem.* **2001**, *66*, 8094.
(44) Schneider, H. J. *Chem. Soc. Rev.* **1994**, *23*, 227.
(45) We assume that the binding of ligands **1** and **2** to CB[7] results in complete dehydration of the CB[7] cavity.
(46) Kim, J.; Jung, I. S.; Kim, S. Y.; Lee, E.; Kang, J. K.; Sakamoto, S.; Yamaguchi, K.; Kim, K. *J. Am. Chem. Soc.* **2000**, *122*, 540.
(47) Morris, G. M.; Huey, R.; Lindstrom, W.; Sanner, M. F.; Belew, R. K.; Goodsell, D. S.; Olson, A. J. *J. Comput. Chem.* **2009**, *30*, 2785.
(48) *Gaussian, version: 09 Revision A.02*; Gaussian Inc., Wallingford, CT, 2004.
(49) Lee, C. T.; Yang, W. T.; Parr, R. G. *Phys. Rev. B* **1988**, *37*, 785.
(50) Tomasi, J.; Mennucci, B.; Cammi, R. *Chem. Rev. (Washington, DC, U. S.)* **2005**, *105*, 2999.
(51) Humphrey, W.; Dalke, A.; Schulten, K. *J. Mol. Graphics* **1996**, *14*, 33.
(52) Vanommeslaeghe, K.; Hatcher, E.; Acharya, C.; Kundu, S.; Zhong, S.; Shim, J.; Darian, E.; Guvench, O.; Lopes, P.; Vorobyov, I.; MacKerell, A. D. *J. Comput. Chem.* **2010**, *31*, 671.
(53) Kim, K. *Chem. Soc. Rev.* **2002**, *31*, 96.
(54) Wyman, I. W.; Macartney, D. H. *Org. Biomol. Chem.* **2010**, *8*, 253.
(55) Scarso, A.; Trembleau, L.; Rebek, J. *Angew. Chem., Int. Ed.* **2003**, *42*, 5499.
(56) Mecozzi, S.; Rebek, J. *Chem.—Eur. J.* **1998**, *4*, 1016.
(57) Ligand **1a** presents a distinct mode of binding to CB[7] as compared to **1b**−**e** and was removed from the series during analysis.
(58) Plyasunov, A. V.; Shock, E. L. *Geochim. Cosmochim. Acta* **2000**, *64*, 439.
(59) Plyasunov, A. V.; Shock, E. L. *J. Chem. Eng. Data* **2001**, *46*, 1016.
(60) MacCallum, J. L.; Moghaddam, M. S.; Chan, H. S.; Tieleman, D. P. *Proc. Natl. Acad. Sci. U.S.A.* **2007**, *104*, 6206.
(61) Baron, R.; Setny, P.; McCammon, J. A. *J. Am. Chem. Soc.* **2010**, *132*, 12091.
(62) Setny, P.; Baron, R.; McCammon, J. A. *J. Chem. Theory Comput.* **2010**, *6*, 2866.
(63) Syme, N. R.; Dennis, C.; Phillips, S. E. V.; Homans, S. W. *ChemBioChem* **2007**, *8*, 1509.
(64) Prabhu, N. V.; Sharp, K. A. *Annu. Rev. Phys. Chem.* **2005**, *56*, 521.
(65) Shimizu, S.; Chan, H. S. *J. Am. Chem. Soc.* **2001**, *123*, 2083.
(66) Bourne, Y.; Radic, Z.; Sulzenbacher, G.; Kim, E.; Taylor, P.; Marchot, P. *J. Biol. Chem.* **2006**, *281*, 29256.
(67) Rasaiah, J. C.; Garde, S.; Hummer, G. *Annu. Rev. Phys. Chem.* **2008**, *59*, 713.
(68) Saenger, W. *Angew. Chem., Int. Ed. Engl.* **1980**, *19*, 344.
(69) Ashbaugh, H. S.; Pratt, L. R. *Rev. Mod. Phys.* **2006**, *78*, 159.
(70) Dill, K. A.; Truskett, T. M.; Vlachy, V.; Hribar-Lee, B. *Annu. Rev. Biophys. Biomol. Struct.* **2005**, *34*, 173.
(71) Lemieux, R. U. *Acc. Chem. Res.* **1996**, *29*, 373.
(72) Syme, N. R.; Dennis, C.; Bronowska, A.; Paesen, G. C.; Homans, S. W. *J. Am. Chem. Soc.* **2010**, *132*, 8682.
(73) Baldwin, R. L. *Proc. Natl. Acad. Sci. U.S.A.* **2012**, *109*, 7310.
(74) Yang, F.; Dearden, D. V. *Isr. J. Chem.* **2011**, *51*, 551.